An Interactive Graphics-Based Model of the Lower Extremity to Study Orthopaedic Surgical Procedures

SCOTT L. DELP, J. PETER LOAN, MELISSA G. HOY, FELIX E. ZAJAC, MEMBER, IEEE, ERIC L. TOPP, AND JOSEPH M. ROSEN

Abstract—**We have developed a model of the human lower extremity to study how surgical changes in musculoskeletal geometry and musculotendon parameters affect muscle force and its moment about the joints. The lines of action of 43 musculotendon actuators were defined based on their anatomical relationships to three-dimensional bone surface representations. A model for each actuator was formulated to compute its isometric force-length relation. The kinematics of the lower extremity were defined by modeling the hip, knee, ankle, subtalar, and metatarsophalangeal joints. Thus, the force and joint moment that each musculotendon actuator develops can be computed for any body position. The joint moments calculated with the model compare well with experimentally measured isometric joint moments.**

We developed a graphical interface to the model that allows the user to visualize the musculoskeletal geometry and to manipulate the model parameters to study the biomechanical consequences of orthopaedic surgical procedures. For example, tendon transfer and lengthening procedures can be simulated by adjusting the model parameters according to various surgical techniques. Results of the simulated surgeries can be analyzed quickly in terms of postsurgery muscle forces and other biomechanical variables. Just as interactive graphics have enhanced engineering design and analysis, we have found that graphics-based musculoskeletal models are effective tools for designing and analyzing surgical procedures.

INTRODUCTION

MUSCLES and tendons actuate movement by developing and transmitting force to the skeleton. When human movement is impaired by disease or trauma, function can sometimes be restored with surgical reconstruction of musculoskeletal structures. For example, patients with muscular spasticity often undergo tendon lengthening and transfer surgeries to correct gait abnormalities. Such surgical procedures, however, often compromise the capacity of the muscles to generate force and moment about the joints. For instance, when a tendon is lengthened or transferred to a new location, the muscle fibers may be too long or too short to generate active force. Lack of sufficient muscle strength or moment arm can leave the patient with weak or dysfunctional limbs. Models of the musculoskeletal system that help to understand the biomechanical consequences of surgically manipulating musculoskeletal structures are needed to analyze difficult surgeries and to design more effective procedures.

The geometry of the musculoskeletal system is complex. Computer display is therefore helpful to visualize the three-dimensional geometric relationships among the muscles and bones, and to understand how these relationships are altered during surgery. Musculoskeletal geometry is important to the function of muscles because it determines the moment arm of each muscle and thus the moment about a joint of a given muscle force. Geometry also determines musculotendon length (i.e., distance from origin to insertion) for a specific body position. Since musculotendon force depends on musculotendon length [1], accurate specification of musculoskeletal geometry is necessary to calculate both musculotendon force and its moment about the joints.

Other investigators have developed models of the lower extremity to evaluate muscular forces and moments during walking [2], kicking [3], and other activities (see [1] for review). In general, these studies emphasize the calculation of muscle forces using optimization theory, but do not focus on musculoskeletal geometry. Models demonstrating the effects of musculoskeletal geometry on musculotendon function exist [4]–[7], but these have not been applied to analyze surgical procedures. Lower-extremity models have been applied to study surgeries such as total hip reconstructions [8], osteotomies [9], [10], and tendon transfers [11]. However, since these models were not implemented on computer graphics workstations, they provided no means to visualize the geometric changes caused by the surgery, nor did they enable the user to graphically alter the model parameters.

The advantages of using interactive graphics to model the musculoskeletal system were first described in 1977 [12]. Since that time, advances in computer and display technology have significantly expanded the potential to visualize and interact with models of musculoskeletal structures. For example, three-dimensional reconstructions from computed tomographic data are now being used to plan total hip reconstructions, osteotomies, and allograph procedures [13]. Wood *et al.* [14] have displayed

Manuscript received July 30, 1989; revised January 13, 1990. This work was supported by the Rehabilitation R & D Service, Department of Veteran Affairs; Aerospace Human Factors Research Division, NASA Ames Research Center, and a NSF Fellowship to S. Delp.

The authors are with the Rehabilitation Research and Development Center (153), VA Medical Center, Palo Alto, CA 94304, and the Department of Mechanical Engineering, Design Division, Stanford University, Stanford, CA 94305.

IEEE Log Number 9036235.

upper-limb musculature as part of their efforts to design prosthetic arm controllers. To help design more effective tendon transfers, others have developed a graphics-based system to simulate hand biomechanics [15], [16]. However, no graphics-based model has been reported to study the biomechanical consequences of surgical reconstructions of the lower extremity.

We have developed a computer graphics-based model to study how surgical changes in musculoskeletal geometry and musculotendon parameters (e.g., optimal muscle-fiber length and tendon slack length) affect the forces and joint moments produced by the lower-extremity muscles. We describe here a model that defines the musculoskeletal geometry and musculotendon parameters for 43 musculotendon actuators in the lower extremity. With this model we can compute each muscle's contribution to the moment about the joint(s) it spans for any body position. We also describe the user interface that allows one to manipulate the musculoskeletal geometry and adjust the model parameters to determine the sensitivity of a surgical outcome to the parameters of a surgical procedure.

Lower-Extremity Model

The lower-extremity model is implemented within a general software system that we have developed to analyze musculoskeletal structures. In this general software system, the particular musculoskeletal structure to be analyzed (e.g., the lower extremity) is specified with several input files. The "bone" file contains lists of the polygons representing the bone surfaces. The "joint" file specifies the kinematic topology of the system and the kinematics of the joints. The kinematics of each joint are specified by six functions, one for each possible degree of freedom (three translations and three rotations). Finally, the "muscle" file contains a list of coordinates that describe each muscle's line of action and the parameters (described below) needed to compute muscle force. Although this general software system can be applied to analyze any musculoskeletal structure, we focus here on our model and analysis of the lower extremity.

Musculoskeletal Geometry

To acquire the bone surface data, we first marked bone surfaces with a mesh of polygons, and then determined the coordinates of the vertices with a Polhemus three-dimensional digitizer. These coordinates were used to display the pelvis, thigh, shank, and foot bones on the computer graphics system (Silicon Graphics, Iris 2400T) as either wireframe objects or Gouraud shaded surfaces. Based on the anatomical landmarks of the bone surface models, we defined the paths (i.e., the lines of action) of 43 musculotendon actuators. Each musculotendon path is represented as a series of line segments. Origin and insertion are necessary landmarks and, in some cases, are sufficient for describing the muscle path (e.g., soleus is represented by a single line segment). In other cases, where the muscle wraps over bone or is constrained by retinacula, intermediate "via points" were introduced to represent the muscle path more accurately (e.g., peroneus longus is represented by a series of six line segments, see Fig. 1). The number of muscle via points can depend on the body position. For example, the quadriceps tendon wraps over the distal femur when the knee is flexed beyond some angle, but not when the knee is extended. Thus, additional via points, called "wrapping points," are introduced for knee flexion angles greater than 90° so that the quadriceps tendon wraps over the bone, rather than passes through the bone, in that range of knee motion.

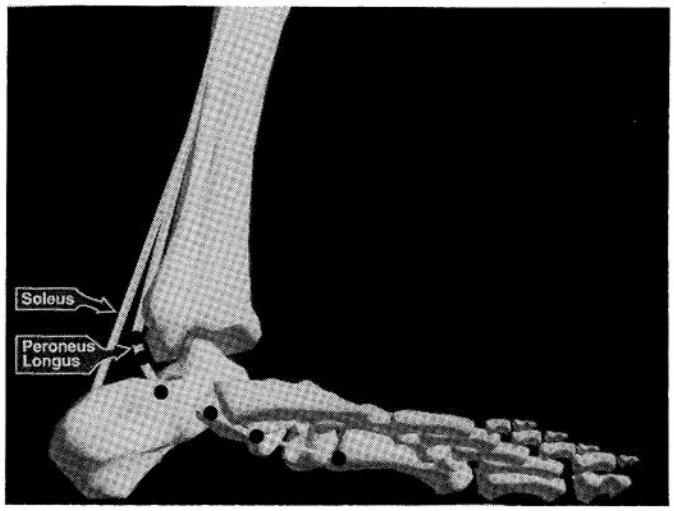

Fig. 1. Three-dimensional representation of the musculotendinoskeletal geometry of the shank, foot, and toes. Some musculotendon actuators are represented as single line segments (e.g., soleus). Others are represented as a series of line segments (e.g., peroneus longus).

On the computer graphics system, we visually compared our muscle paths with paths defined by a commonly used set of muscle coordinates [17]. In the anatomical position, the paths are similar. However, interactively changing the skeletal configuration revealed that several muscle paths reported by Brand *et al.* [17] (e.g., iliacus, gluteus maximus, and sartorius) passed through the bones or deeper muscles. This occurred because each muscle path reported by Brand *et al.* is defined by only two points that were measured on cadavers in the anatomical position. Displaying the muscle paths along with the bone surface models was helpful because it clearly showed where muscle via points and wrapping points were needed to properly constrain the musculotendon paths. We also compared moment arms calculated from our muscle paths with measurements we took from cadavers and from cross-sectional anatomy texts [18], as well as with moment arms reported in the literature (e.g., [11], [19], [20]). These comparisons showed that our muscle paths are anatomically correct, and generate moment arms that are consistent with previous investigations.

Moment arms and musculotendon lengths are calculated with the following method. First, all muscle coordinates are transformed to a common reference frame. Then, moment arms (ma) and musculotendon lengths (ℓ^{MT}) are computed as shown in Fig. 2. Equation (1)

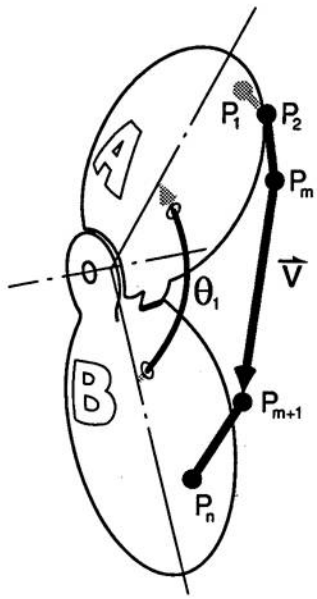

Fig. 2. Calculation of moment arm and musculotendon length for a muscle crossing a revolute joint. Coordinates P_1 through P_n define the muscle path. P_1 through P_m are fixed in body A; P_{m+1} through P_n are fixed in body B. Thus, $\vec{V}$ (where $\vec{V} = P_{m+1} - P_m$) is the only muscle segment that changes length as the joint is flexed. In general, three angles, $\theta_i (i = 1, 2, 3)$ are needed to characterize the orientation of body A relative to body B. Only one angle, θ_1, is needed for a revolute joint. The moment arm (ma) for each orientation angle is given by:

$$ma = \partial \ell / \partial \theta_i, \quad \text{where } \ell = |\vec{V}|. \tag{1}$$

Musculotendon length (ℓ^{MT}) is given by:

$$\ell^{MT} = \sum_{i=1}^{n-1} |P_{i+1} - P_i| \tag{2}$$

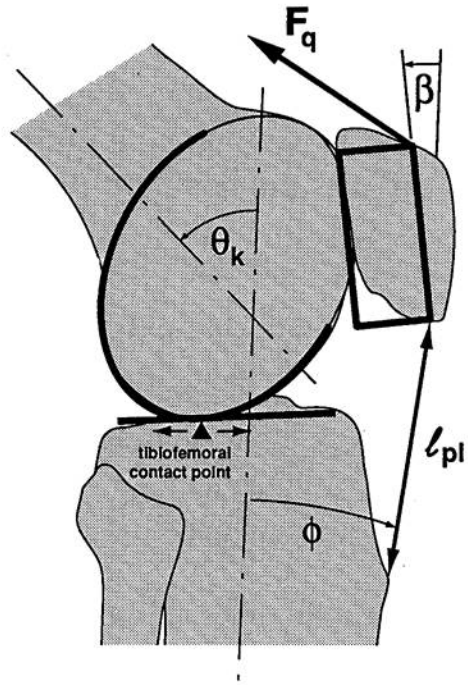

Fig. 3. Geometry for determining knee moments and kinematics in the sagittal plane. θ_k is the knee angle; ϕ is the patellar ligament angle; β is the angle between the patella and the tibia; F_q is the quadriceps force; ℓ_{pl} is the length of the patellar ligament. From these kinematics, the moment of the quadriceps force about the instant center of knee rotation can be computed.

(caption for Fig. 2) provides a computationally consistent, mechanically correct method to determine moment arms for all types of joints. Equation (1) is equivalent to computing moment arms with a vector cross product [4] for ball-and-socket and revolute joints. For a planar joint that includes kinematic constraints (e.g., our knee model), (1) gives the moment arm of a muscle about the instant joint center as determined from the joint kinematics.

Joint Models

We modeled the lower extremity as seven rigid-body segments: 1) pelvis, 2) femur, 3) patella, 4) tibia/fibula, 5) talus, 6) foot (comprising the calcaneus, navicular, cuboid, cuneiforms, and metatarsals), and 7) toes (phalanges), with reference frames fixed in each segment. The relative motion of these segments is defined by models of the hip, knee, ankle, subtalar, and metatarsophalangeal joints.

We characterized the hip as a ball-and-socket joint. The transformation between the pelvic and femoral reference frames is thus determined by successive rotations of the femoral frame about three orthogonal axes fixed in the femoral head.

We modified a planar model of the knee [20] to characterize the knee extensor mechanism. This single-degree-of-freedom model accounts for the kinematics of both the tibiofemoral joint and the patellofemoral joint in the sagittal plane as well as the patellar levering mechanism. We specified the transformations between the femoral, tibial, and patellar reference frames as functions of the knee angle. Tibiofemoral kinematics were determined as follows. The femoral condyles were represented as an ellipse; the tibial plateau was represented as a line segment (Fig. 3). The transformation from the femoral reference frame to the tibial reference frame was then determined so that the femoral condyles remain in contact with the tibial plateau throughout the range of knee motion. The tibiofemoral contact point depends on the knee angle and was specified according to data reported by Nisell *et al.* [21]. Assuming that the length of the patellar ligament (ℓ_{pl} in Fig. 3) is constant, the angle between the patellar ligament and the tibia (ϕ in Fig. 3) determines the translation vector from the tibial reference frame to the patellar reference frame [22]. Rotation of the patella with respect to the tibia (β in Fig. 3) was specified according to experimental measurements of patellar rotation [22]. Moment arms calculated from these kinematics correspond closely to moment arms that have been measured experimentally (see [22a] for comparison).

We modeled the ankle, subtalar, and metatarsophalangeal joints as frictionless revolutes (Fig. 4). Isman and Inman [23] have described the location and orientation of axes for each of these joints. When displayed, these axes produced realistic motion of the ankle and subtalar joints (i.e., the bone surface models did not collide or disarticulate), but unrealistic motion of the metatarsophalan-

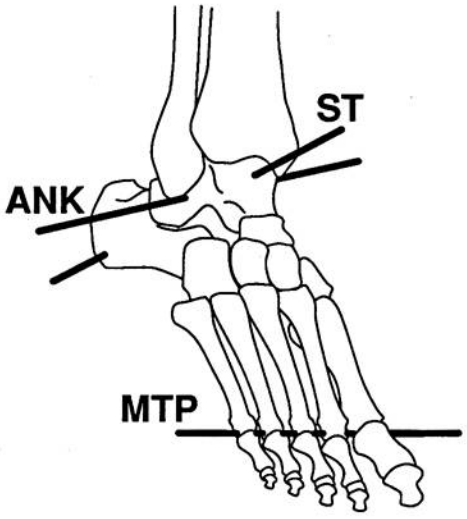

Fig. 4. The ankle (ANK), subtalar (ST), and metatarsophalangeal (MTP) joints are modeled as revolute joints with axes oriented as shown.

geal joint (the phalanges separated from the metatarsals). We therefore rotated the metatarsophalangeal axis ($-8°$ about a vertical axis) to minimize disarticulation of that joint.

Musculotendon Actuator Model

To compute musculotendon force as a function of musculotendon length, we formulated a specific model for each musculotendon actuator. Each specific model was formed from a generic model [1] that accounts for the static properties of both muscle [24] and tendon [25] (Fig. 5). When the generic model is scaled by a muscle's peak isometric force (F_o^M), optimal muscle-fiber length (ℓ_o^M), pennation angle (α), and tendon slack length (ℓ_s^T), the force-length relation of a specific musculotendon actuator can be computed [1]. Values for muscle physiological cross-sectional area, which scale F_o^M [26], were taken from the literature [27], [28]. Values for ℓ_o^M and α, which scale the range of lengths over which a musculotendon actuator develops force, were taken from Wickiewicz *et al.* [28]. For muscles not reported by Wickiewicz *et al.*, we used muscle-fiber lengths and pennation angles measured by Friederich and Brand in the anatomical position [28a].

Since no experimental data exist for tendon slack length (i.e., tendon length beyond which force develops), one application of our model was to estimate ℓ_s^T for each actuator. Tendon slack length includes both the length of free tendon and the length of tendon internal to the muscle belly (aponeurotic tendon). When muscle paths are specified, as above, ℓ_s^T determines the joint angles where a musculotendon actuator develops force [1], [4]. We specified values for ℓ_s^T based on the following two criteria [4]. First, assuming that passive muscle contributes to the joint moment (called "passive moment") only when the muscle fibers are longer than ℓ_o^M, we selected ℓ_s^T so that actuators were slightly longer than ℓ_o^M at joint angles corresponding to the onset of *in vivo* passive moment measured at the hip [29], knee [30], [31], and ankle [32]. Second,

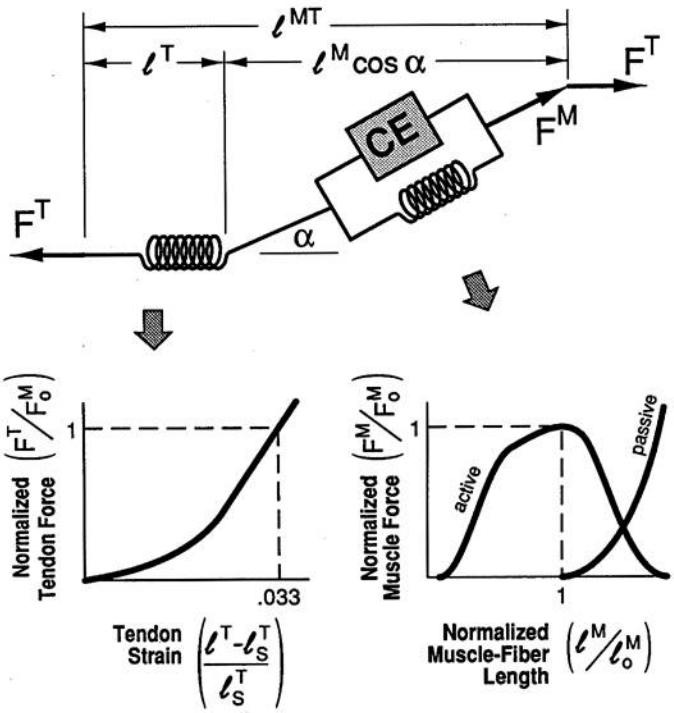

Fig. 5. Musculotendon actuator model. The isometric properties of muscle are represented by an active contractile element (CE) in parallel with a passive elastic element. Isometric muscle force is assumed to be the sum of muscle force when it is inactive (passive) and when it is excited (active). The muscle is in series with tendon, which is represented by a nonlinear elastic element. The forces in muscle (F^M) and tendon (F^T) are normalized by peak isometric muscle force (F_o^M). Tendon length (ℓ^T) and muscle-fiber length (ℓ^M) are normalized by optimal muscle-fiber length (ℓ_o^M). Note that: $\ell^{MT} = \ell^T + \ell^M (\cos\alpha)$ and $F^T = F^M (\cos\alpha)$ where ℓ^{MT} is the musculotendon length and α is the pennation angle. L_s^T is the tendon slack length. For a given musculotendon length and activation level the model determines musculotendon force.

since ℓ_s^T determines the joint angle where an actuator develops peak active joint moment (i.e., moment of active muscle force about a joint), we adjusted ℓ_s^T so that the total active moment about each joint peaked at a joint angles corresponding to *in vivo* measurements of joint moment (e.g., see Fig. 6 below).

Model Output

By combining the musculoskeletal geometric data, joint models, and musculotendon models, we are able to compute the force and joint moment that each muscle can develop for any body position. For a given body position we compute musculotendon length and moment arm with the equations given in Fig. 2. Using the musculotendon actuator models, we then compute the maximum (i.e., fully activated) isometric muscle force at the computed musculotendon length. The joint moment for each muscle is then computed as the product of the tendon force and the moment arm.

We summed the active joint moments exerted by all muscles, and compared these total computed moments to active joint moments measured during maximum voluntary isometric contractions. For example, Fig. 6 compares the total active plantarflexion moment computed with the model to the moment measured during maximum

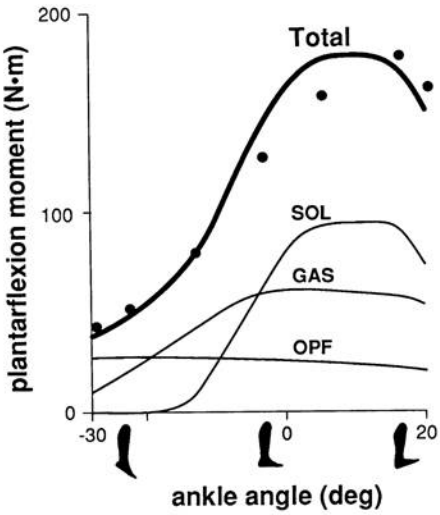

Fig. 6. Comparison of computed and experimental active plantarflexion moments. Computed moments of soleus (SOL), medial and lateral gastrocnemius (GAS), and the other plantarflexors (OPF) were summed to produce to total computed moment (thick-solid line). The total computed moment, with muscles fully activated, compared well with plantarflexion moments measured during maximum voluntary isometric contractions (large dots) [33].

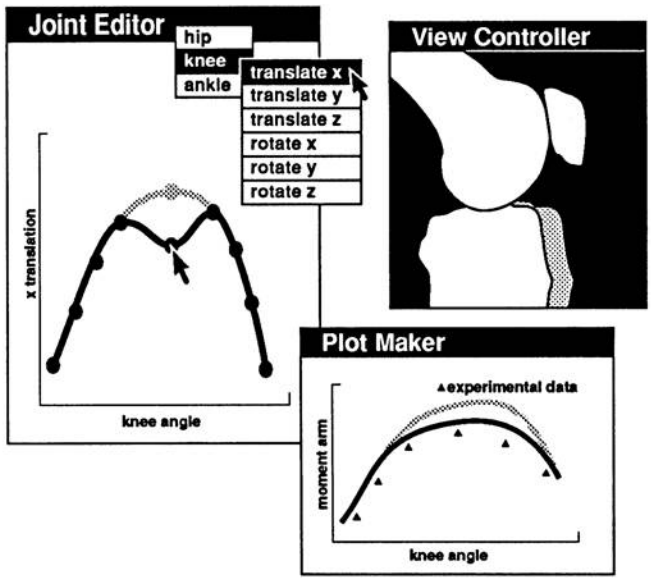

Fig. 7. Graphic manipulation of knee kinematics. In the left window (joint editor), the user can alter the splines that define joint kinematics by moving the spline's control points. In this example, the spline controlling X-translation of the tibia with respect to the femur is altered. The resulting motion of the knee can be observed in the view controller window (upper right). The effect of these kinematic changes on the knee moment arm can also be plotted and compared to experimental data (lower right).

voluntary isometric contraction of the ankle plantarflexors [33]. The computed ankle moment corresponds closely with the measured plantarflexion moment, both with the knee extended and flexed. Similar to Fig. 6, we found excellent agreement between computed joint moments and moments measured at the hip [19], [34], [35], knee [36], ankle [33], [37], and subtalar [38] joints. (See [22a] for comparisons of computed and measured joint moments.)

Interacting with the Model

An effective user interface has been critical in both developing and using the lower-extremity model. Four software tools help the user to modify and analyze the musculoskeletal model.

The "view controller" allows the user to rotate, scale, and translate the model into any viewing perspective. The joints can also be flexed using a mouse to examine the joint motion and to see how the muscle paths change with joint angle. To improve display speed, the model is represented as a wireframe object during these transformations. Once a desired view has been reached, the model can be rendered as a Gouraud shaded image to enhance visualization.

The "joint editor" enables the user to graphically manipulate the kinematics of any joint. For example, the user may choose to display the kinematic functions (cubic splines) that define the relative motion of the femur and tibia. These functions can then be changed by moving each spline's control points with a mouse. The resulting motion can then be observed by flexing and extending the knee. The quantitative effects of these kinematic changes can also be displayed (Fig. 7). Graphic manipulation of joint kinematics is an efficient way to refine the model parameters to match experimental data and to alter the joint motion according to surgical procedures.

The "muscle editor" gives access to every parameter that describes a muscle. The muscle paths can be altered by first selecting a muscle from a screen menu and then choosing its origin, insertion, or one of the muscle via points. The chosen muscle point can then be moved in the X, Y, and Z directions. An algorithm assists the user in attaching a muscle point to the bone by first finding the surface polygon closest to the muscle point and then moving the muscle point toward that polygon. At any time, a muscle point can be added or deleted, or the muscle can be restored to its original path. The muscle paths and bone geometry are displayed throughout the musculotendon path planning process. Each of the musculotendon parameters (F_o^M, ℓ_s^T, ℓ_o^M, α, activation) can be changed by using a mouse to select a parameter from a menu that lists all the parameters, and then typing in a new parameter value.

The "plot maker" allows the user to display the mechanical effects of changing a joint or muscle. For example, the user may plot the effect of changing a muscle's path on its moment arm or length. Or, the effect of changing an actuator's tendon slack length (ℓ_s^T) or muscle-fiber length (ℓ_o^M) on muscle force may be plotted for a range of joint motion. To specify a plot, the user first chooses the Y-axis variable (e.g., force, moment, length, moment arm) and then the X-axis variable (joint motion). Next, the user selects a muscle, or set of muscles, from menus that group the muscles according to their functions. Finally, the user may specify the angles of the adjacent joints (e.g., the hip may be flexed at a specific angle while the effects of knee flexion on joint moment are calculated). Fig. 8 shows the menus used to specify the plots, alter the musculotendon parameters, and specify the joint an-

gles along with an example of the graphical output (soleus force versus ankle angle for three values of ℓ_s^T and ℓ_o^M).

Surgery Simulation

To determine how a planned surgical procedure affects muscle force and joint moment, we adjust the model's muscle paths, muscle strengths, muscle-fiber lengths, and tendon lengths according to a specific surgical technique. For example, to simulate the mechanical effects of an Achilles tendon lengthening with concomitant anterior transfer of the tibialis posterior (a procedure commonly performed to correct an equinovarus deformity [39]), we increase the model's Achilles tendon length and graphically detach the tendon of tibialis posterior from its insertion on the navicular bone, and reroute its path to insert on the dorsum of the foot. The results of this simulated surgery are then displayed as plots of presurgery and postsurgery plantarflexion and dorsiflexion moments versus ankle angle (Fig. 9).

Notice that the magnitude and the shape of the plantarflexion moment versus ankle angle curve are changed by the surgery (cf. purple and blue lines in Fig. 9). Two factors cause the significant decrease (65% at 0°) in the ankle plantarflexion moment. First, after surgery, the tibialis posterior does not contribute to the plantarflexion moment since it crosses the ankle joint anteriorly. Second, and more importantly, increasing the Achilles tendon length changes the ankle angle at which both the gastrocnemius and soleus produce maximum force. This combination of effects not only decreases the magnitude, but also shifts the angle of the peak moment toward greater dorsiflexion. We found that the plantarflexion moment is extremely sensitive to changes in Achilles tendon length. This may explain why it is clinically difficult to maintain plantarflexion strength after Achilles tendon lengthening procedures [40].

In this particular surgery simulation, the postsurgery dorsiflexion moment is greater than the presurgery moment, but only in the range of ankle plantarflexion ($-30°$ to 0°) (cf. red and green lines in Fig. 9). The significant increase in dorsiflexion moment in the range of ankle plantarflexion (100% at $-30°$) can be attributed to the large force developed by tibialis posterior in that range. Presurgery and postsurgery dorsiflexion moments are equal in the range of ankle dorsiflexion (0° to 20°) because the fibers of tibialis posterior are too short to develop force in dorsiflexion.

The primary reason for transferring the tibialis posterior is to correct the varus component of the equinovarus deformity. Indeed, the varus moment will be decreased by this transfer since, after surgery, the tendon passes lateral to the subtalar joint. However, in this particular simulation, tibialis posterior does not generate a corrective valgus moment when the ankle is dorsiflexed since its fibers are too short to develop force in dorsiflexion. If the attachment of the tendon were moved distally on the metatarsal, or if the tendon were shortened, the tibialis posterior would then generate force, and thus valgus moment, over the full range of ankle motion. Such variations in the surgical procedure are easily explored on the computer graphics system.

Sensitivity Results

We performed a sensitivity study to understand how the musculotendon parameters and musculoskeletal geometry affect muscle force. The joint angle at which a muscle develops peak force (θ_o) depends on tendon slack length (ℓ_s^T) (Fig. 8, left plot) and optimal muscle-fiber length (ℓ_o^M) (Fig. 8, right plot). To determine the sensitivity of muscle force to ℓ_s^T and ℓ_o^M we varied these parameters and determined the change in the *joint angle* at which each actuator develops peak force ($\Delta\theta_o$). This change in the joint angle also depends on the actuator's moment arm (ma), since $\partial\theta = \partial\ell/\text{ma}$ (see caption for Fig. 2). The change in joint angle at which four actuators develop peak force resulting from a 5% change in ℓ_s^T and ℓ_o^M is shown in Fig. 10.

We found that the angle of peak force (θ_o) is more sensitive to a change in tendon length for actuators with high ratios of tendon length to moment arm (ℓ_s^T/ma) than for actuators with low ℓ_s^T/ma ratios (Fig. 10, open bars). For example, changing the ℓ_s^T of gastrocnemius by 5% shifted the joint angle of peak force by 38°, whereas a 5% change in the ℓ_s^T of gracilis shifted the angle by only 6°. Similarly, the angle of peak force is more sensitive to a change in optimal muscle-fiber length for actuators with long fibers relative to moment arm (i.e., high ℓ_o^M/ma ratios) than for actuators with low ℓ_o^M/ma ratios (Fig. 10, filled bars). For instance, a 5% change in the ℓ_o^M of gracilis shifted the joint angle of peak force by 16° while the same percentage change shifted gastrocnemius force by only 2°. In general, θ_o is more sensitive to ℓ_s^T than ℓ_o^M since $\ell_s^T/\ell_o^M > 1$ for most actuators (cf. magnitude of open and filled bars).

The range of joint angles over which an actuator develops active force increases with the ratio of its optimal fiber length to its moment arm (i.e., range increases with ℓ_o^M/ma). Hence, muscles with small ℓ_o^M/ma ratios (e.g., gastrocnemius, soleus, rectus femoris) develop active force over a relatively limited range of motion (e.g., soleus develops active force over only 50° of ankle motion). Since ℓ_o^M has been measured for many muscles in the lower extremity [28], and given that the muscle paths presented here yield reasonable moment arms, we expect that the calculated range of motion over which each actuator develops active force is fairly accurate.

Since no experimental measurements of ℓ_s^T have been reported, it is important to assess the adequacy of our ℓ_s^T estimates. We have shown that the angle of peak muscle force is most sensitive to ℓ_s^T for actuators with high ℓ_s^T/ma ratios (e.g., gastrocnemius, soleus, rectus femoris). We have also shown that actuators with low ℓ_o^M/ma ratios develop force over a limited range of motion. Consequently, ℓ_s^T must be specified accurately for actuators with both high ℓ_s^T/ma ratios and low ℓ_o^M/ma ratios (i.e., actuators with

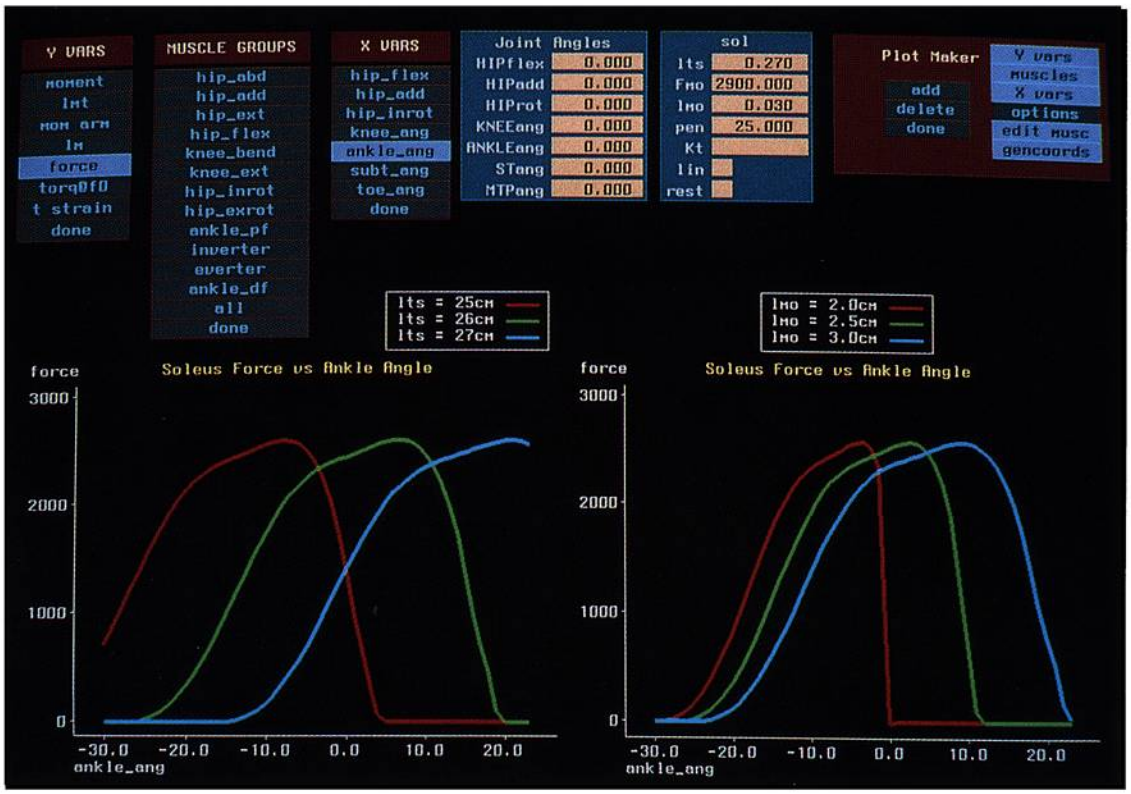

Fig. 8. Display highlighting the user interface. The menus along the top allow the user to specify the plotting parameters. The plots below show soleus active force versus ankle angle for three values of tendon slack length (ℓ_s^T) (left plot) and optimal muscle-fiber length (ℓ_o^M) (right plot). Negative ankle angles indicate plantarflexion; positive angles indicate dorsiflexion. Note that the angle of peak soleus force changed by 30° for a 2 cm change in ℓ_s^T (left plot). Decreasing ℓ_o^M not only changed the angle of peak force, but also decreased the range of ankle angles over which soleus develops active force (right plot).

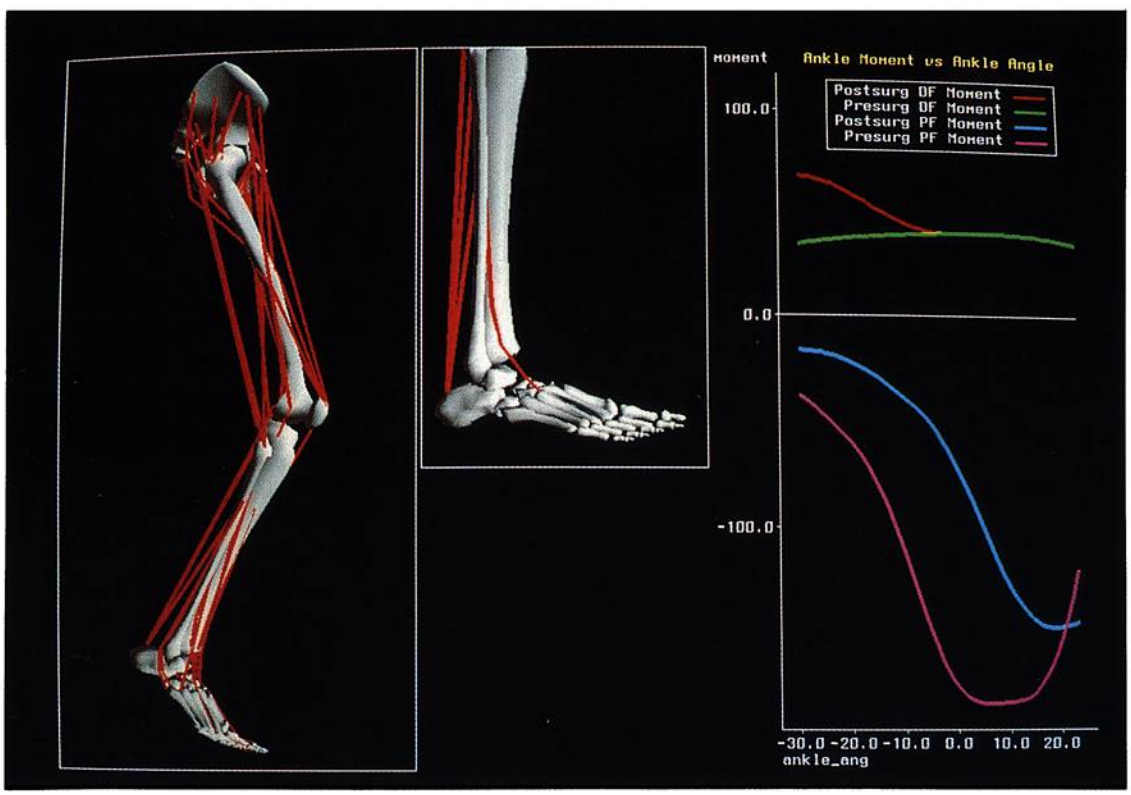

Fig. 9. Display from a simulated surgery in which the Achilles tendon was lengthened (1 cm) and the tendon of tibialis posterior was transferred to the base of the third metatarsal. The left postsurgery musculoskeletal geometry. The plot on the right shows presurgery and postsurgery ankle plantarflexion and dorsiflexion moments (in N-m) versus ankle angle. Positive (negative) ankle angles and moments indicate dorsiflexion (plantarflexion). Postsurgery dorsiflexion moment is increased significantly, but only in the range of ankle plantarflexion (cf. red and green lines). Postsurgery plantarflexion moment is greatly decreased (cf. purple and blue lines).

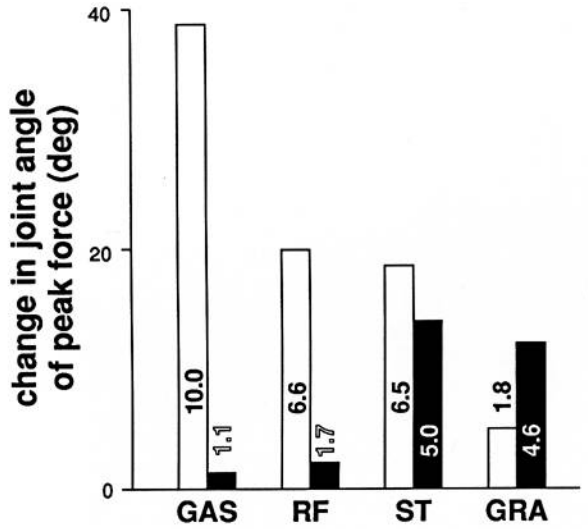

Fig. 10. Change in joint angle at which four musculotendon actuators [gastrocnemius (GAS), rectus femoris (RF), semitendinosus (ST) and gracilis (GRA)] develop peak force resulting from a 5% change in tendon slack length (ℓ_s^T) (open bars) and optimal muscle-fiber length (ℓ_o^M) (filled bars). The number associated with each open (filled) bar is the ℓ_s^T/ma (ℓ_o^M/ma) ratio of that actuator. The moment arms (ma) were computed at the ankle (GAS), knee (RF and ST), and hip adduction (GRA) angles at which these actuators develop peak force. Note that actuators with high ℓ_s^T/ma ratios (ℓ_o^M/ma ratios) are most sensitive to a change in tendon length (fiber length).

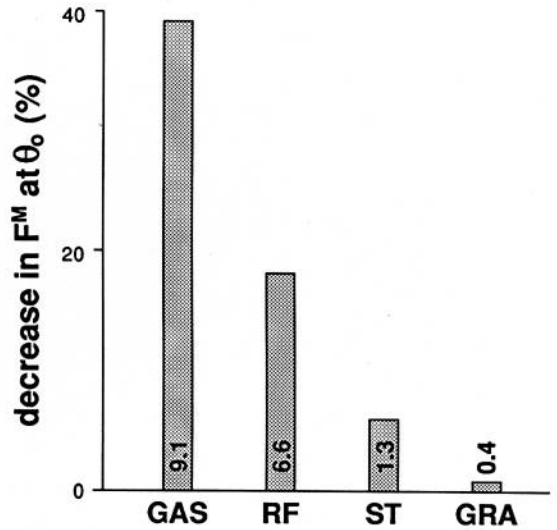

Fig. 11. Decrease in muscle force (F^M) at the joint angle of peak force (θ_o) resulting from a 5% increase in tendon slack length(ℓ_s^T). The numbers associated with the bars for gastrocnemius (GAS), rectus femoris (RF), semitendinosus (ST), and gracilis (GRA) are the tendon slack length to muscle-fiber length ratios (ℓ_s^T/ℓ_o^M) for each actuator. Note that the magnitude of the muscle force is significantly more sensitive to a change in tendon length for actuators with high ℓ_s^T/ℓ_s^M ratios.

high ℓ_s^T/ℓ_o^M ratios), so that active force is developed in the physiologic range of motion. Since the modeled actuators indeed develop force in the physiologic range of motion, we are confident in the estimates of ℓ_s^T for muscles with high ℓ_s^T/ℓ_o^M ratios. We are less confident in our estimates of ℓ_s^T for muscles with low ℓ_s^T/ℓ_o^M ratios (e.g., sartorius, gracilis, iliacus); however, the force developed by these muscles is less sensitive to ℓ_s^T and thus accurate estimates of ℓ_s^T are less critical.

To study how increasing tendon length influences the *magnitude* of the forces generated by the muscles, we increase the ℓ_s^T of each actuator by 5% and measured the decrease in the force at the angle of peak force (θ_o). Fig. 11 shows that the magnitude of the force developed at θ_o by actuators with large ratios of tendon length to fiber length (ℓ_s^T/ℓ_o^M) is much more sensitive to a change in tendon length. For example, gastrocnemius force decreased by 40% at θ_o for a 5% (2.0 cm) increase in ℓ_s^T, whereas gracilis force decreased only 1% at θ_o for a 5% (0.7 cm) increase in ℓ_s^T. These results indicate that, in an actual surgery, a much larger decrease in force will be realized by lengthening the tendons of muscles with high ℓ_s^T/ℓ_o^M ratios (the ankle actuators) than by lengthening the tendons of muscles with low ℓ_s^T/ℓ_o^M ratios (the hip actuators).

Discussion

It is important to discuss the assumptions and limitations of our model. First, we have simplified the knee model to represent motion in the sagittal plane only. While this does not account for rotation of the tibia about its longitudinal axis near full extension [41], or varus/valgus rotation, these nonplanar rotations are small compared to motion in the sagittal plane [20]. Since our objective was to determine the effects of knee flexion and extension on musculotendon excursions, forces, and moments, the sagittal-plane model is adequate. We have also idealized the ankle and subtalar joints as fixed-axis revolutes. This is a reasonable assumption for the ankle, but the subtalar joint has more complex kinematic characteristics [42]. Thus, we are fairly confident in the ankle moment calculations, but less confident in the computed subtalar moments. Since our software system allows for six degrees of freedom between any two bones, more complex joint models can easily be incorporated into the lower-extremity model.

Second, the musculoskeletal geometry and musculotendon parameters have been specified for only a single, nominal subject. However, there is a paucity of experimental data to indicate how the musculotendon parameters vary among subjects with different musculoskeletal geometry (i.e., different moment arms and body-segment lengths). If we assume that the range of joint angles over which each actuator develops active force is relatively constant among individuals, then ℓ_o^M would scale with the moment arm (ma) since the ℓ_o^M/ma ratio determines the range of joint angles over which active force is developed [4]. Furthermore, if we assume that the joint angle at which each actuator develops peak force is also subject independent, we would expect ℓ_s^T to vary to accommodate the change in musculotendon length in subjects with different body-segment lengths.

A third limitation is display speed. Our current workstation takes nearly two seconds to render a shaded image of the lower extremity ($\approx$4000 polygons). Hence, we can only interact with the model in wireframe mode. Wire-

frame images are visually ambiguous and sometimes difficult to interpret. However, recent advancements in graphics workstations make it possible to animate complex shaded images in real time. Once we convert our software to run on such a workstation (Silicon Graphics, 4D/25), we will be able to manipulate our model as a shaded image. This will significantly enhance our ability to visualize the model geometry and to understand the simulation results.

In the past, biomechanists have represented muscles as single lines from origin to insertion [2], [3], [17] and resorted to physical models, such as elastic threads attached to skeletons, to visualize the muscle paths [7], [43]. The ability to manipulate computer-generated images of musculoskeletal structures has allowed us to define more accurate musculotendon paths for all the major lower-extremity actuators, and to efficiently change these paths to study the biomechanical consequences of surgical reconstructions.

Display of the bone surfaces was also helpful in developing the joint kinematic models. Although the knee model has only one degree of freedom, there are five constraint functions that specify the relative motion of the femur, tibia, and patella. The ability to graphically alter these constraint functions (Fig. 7) and then view the motion of the knee allowed us to quickly refine the knee model. Dynamic display was also helpful to position and orient the axes for the ankle, subtalar, and metatarsophalangeal joints.

The combined effects of musculoskeletal geometry and musculotendon parameters on the joint moment versus joint angle curve of a muscle are complex. We have found, however, that interacting with our model facilitates rapid discovery of how surgical manipulations of musculotendinoskeletal structures affect the moment generating capacity of the muscles. For example, in a few minutes, one can explore the effects of transferring the insertion of the rectus femoris to the tendon of sartorius (a procedure preformed to correct stiff-legged gait [44]) on the knee flexion/extension moments. Further interaction with the model allows one to determine the sensitivity of the knee and hip moments to the exact location of rectus femoris attachment. Since the graphical mode of interaction eliminates the need for the user to focus on the model's mathematical basis, it can be used not only to analyze surgical procedures, but also to train surgeons.

We have planned several enhancements to the model. In addition to simulating tendon transfers, we plan to analyze total hip replacements to study the effects of prosthesis design and surgical technique on the hip muscular forces. We also plan to implement the model within a standard windowing environment (X windows) to improve software portability. We are currently extending the software so that experimental and simulated human-movement data can be used to drive an animated display of lower-extremity movement. This enhancement will allow us to study the function of muscles during complex activities such as walking and bicycling.

Acknowledgment

We thank D. Stredney for providing the shank and foot bone data. We gratefully acknowledge the assistance of D. Delp, S. Fisher, and E. Bleck.

Note: The exact anatomical locations of the reference frames and muscle paths, and the musculotendon parameters are available by writing to S. Delp.

References

[1] F. E. Zajac, "Muscle and tendon: Properties, models, scaling, and application to biomechanics and motor control," in *CRC Critical Rev. in Biomed. Eng.*, J. Bourne, Ed. Boca Raton, FL: CRC Press, vol. 17, issue 4, 1989, pp. 359–411.

[2] D. E. Hardt, "Determining muscle forces in the leg during normal human walking—an application and evaluation of optimization methods," *J. Biomech. Eng.*, vol. 100, pp. 72–78, 1978.

[3] H. Hatze, "The complete optimization of a human motion," *Math. Biosci.*, vol. 28, pp. 99–135, 1976.

[4] M. G. Hoy, F. E. Zajac, and M. E. Gordon, "A musculoskeletal model of the human lower extremity: the effect of muscle, tendon, and moment arm on the moment-angle relationship of musculotendon actuators at the hip, knee, and ankle," *J. Biomech.*, vol. 23, pp. 157–159, 1990.

[5] H. van Mameran and J. Drukker, "Attachment and composition of skeletal muscles in relation to their function," *J. Biomech.*, vol. 12, pp. 859–867, 1979.

[6] J. M. Mansour and J. M. Pereira, "Quantitative functional anatomy of the lower limb with application to human gait," *J. Biomech.*, vol. 20, pp. 51–58, 1987.

[7] M. R. Pierrynowski and J. B. Morrison, "A physiological model for the evaluation of muscular forces in human locomotion: Theoretical aspects," *Math Biosci.*, vol. 75, pp. 69–101, 1985.

[8] R. C. Johnston, R. A. Brand, and R. D. Crowninshield, "Reconstruction of the hip—a mathematical approach to determine optimum geometric relationships," *J. Bone Joint Surg.*, vol. 61-A, pp. 639–652, 1979.

[9] R. A. Brand and D. R. Pedersen, "Computer modeling of surgery and a consideration of the mechanical effects of proximal femoral osteotomies," in *The Hip*, R. W. Welch Ed. St. Louis: C. V. Mosby, 1984, pp. 193–210.

[10] S. L. Delp, E. E. Bleck, F. E. Zajac, and G. Bollini, "Biomechanical analysis of the Chiari pelvic osteotomy: preserving hip abductor strength," *Clin. Orth. Rel. Res.*, vol. 254, pp. 189–198, 1990.

[11] J. Dul, R. Shiavi and N. E. Green, "Simulation of tendon transfer surgery," *Eng. Med.*, vol. 14, pp. 31–38, 1985.

[12] R. Williams and A. A. Seireg, "Interactive computer modeling of the musculoskeletal system," *IEEE Trans. Biomed. Eng.*, vol. BME-24, pp. 213–219, 1977.

[13] S. B. Murphy, P. K. Kijewski, M. B. Millis, J. E. Hall, S. R. Simon, and H. P. Chandler, "The planning of orthopaedic reconstructive surgery using computer-aided simulation and design," *Comp. Med. Imag., Graphics*, vol. 12, pp. 33–45, 1988.

[14] J. E. Wood, S. G. Meek, and S. C. Jacobsen. "Quantification of human shoulder anatomy for prosthetic arm control—I. surface modelling," *J. Biomech.*, vol. 22, pp. 273–292, 1989.

[15] W. L. Buford and D. E. Thompson, "A system for three-dimensional interactive simulation of hand biomechanics," *IEEE Trans. Biomed. Eng.*, vol. BME-34, pp. 444–453, 1987.

[16] D. E. Thompson and D. J. Giurintano, "A kinematic model of the flexor tendons of the hand," *J. Biomech.*, vol. 22, pp. 327–334, 1989.

[17] R. A. Brand, R. D. Crowninshield, C. E. Wittstock, D. R. Pederson, C. R. Clark, and F. M. van Krieken, "A model of lower extremity muscular anatomy," *J. Biomech. Eng.*, vol. 104, pp. 304–310, 1982.

[18] A. C. Eycleshymer and D. M. Shoemaker, *A cross section anatomy*. New York: Appleton-Crofts, 1970.

[19] G. Nemeth, J. Ekholm, U. P. Arborelius, K. Harms-Ringdahl, and K. Schuldt, "Influence of knee flexion on isometric hip extensor strength," *Scand. J. Rehabil. Med.*, vol. 15, pp. 97–101, 1983.

[20] G. T. Yamaguchi and F. E. Zajac, "A planar model of the knee joint to characterize the knee extensor mechanism," *J. Biomech.*, vol. 22, pp. 1–10, 1989.

[21] R. Nisell, G. Nemeth, and H. Ohlsen, "Joint forces in extension of the knee," *Acta Orthop. Scand.*, vol. 57, pp. 41-46, 1986.
[22] T. M. G. J, Van Eijden, W. de Boer, and W. A. Weijs, "The orientation of the distal part of the quadriceps femoris muscle as a function of the knee flexion-extension angle," *J. Biomech.*, vol. 18, pp. 803-809, 1985.
[22a] S. L. Delp, "A computer-graphics system to analyze and design musculoskeletal reconstructions of the lower limb," Ph.D. dissertation, Stanford Univ., Stanford, CA, 1990.
[23] V. T. Inman, *The Joints of the Ankle*. Baltimore, MD: Williams & Wilkins, 1976.
[24] A. M. Gordon, A. F. Huxley, and F. J. Julian, "The variation in isometric tension with sarcomere length in vertebrate muscle fibers," *J. Physiol.*, vol. 184, pp. 170-192, 1966.
[25] S. S.-Y. Woo, M. A. Gomez, Y.-K. Woo, and W. H. Akeson, "Mechanical properties of tendons and ligaments. II. The relationships of immobilization and exercise on tissue remodeling," *Biorheology*, vol. 19, pp. 397-408, 1982.
[26] S. A. Spector, P. F. Gardiner, R. F. Zernicke, R. R. Roy, and V. R. Edgerton, "Muscle architecture and force-velocity characteristics of cat soleus and medial gastrocnemius: implications of neural control," *J. Neurophysiol.*, vol. 44, pp. 951-960, 1980.
[27] R. A. Brand, D. R. Pedersen, J. A. Friederich, "The sensitivity of muscle force predictions to changes in physiologic cross-sectional area," *J. Biomech.*, vol. 19, pp. 589-596, 1986.
[28] T. L. Wickiewicz, R. R. Roy, P. L. Powell, and V. R. Edgerton, "Muscle architecture of the human lower limb," *Clin. Orthop. Rel. Res.*, vol. 179, pp. 275-283, 1983.
[28a] J. A. Friederich and R. A. Brand, "Muscle fiber architecture in the human lower limb," *J. Biomed.*, vol. 23, pp. 91-95, 1990.
[29] Y. S. Yoon and J. M. Monsour, "The passive elastic moment at the hip," *J. Biomech.*, vol. 15, pp. 905-910, 1982.
[30] Y. F. Heerkens, R. D. Woittiez, P. A. Huijing, A. Huson, G. J. Ingen Schenau, and R. H. Rozendal, "Passive resistance of the human knee: the effect of remobilization," *J. Biomed. Eng.*, vol. 9, pp. 69-76, 1987.
[31] J. M. Mansour and M. L. Audu, "The passive elastic moment at the knee and its influence on human gait," *J. Biomech.*, vol. 19, pp. 369-373, 1986.
[32] S. Siegler, G. D. Moskowitz, and W. Freedman, "Passive and active components of the internal moment developed about the ankle during human ambulation," *J. Biomech.*, vol. 17, pp. 647-652, 1984.
[33] D. Sale, J. Quinlan, E. Marsh, A. J. McComas, and A. Y. Belanger, "Influence of joint position on ankle plantarflexion in humans," *J. Appl. Physiol.: Respirat. Environ. Exer. Physiol.*, vol. 52, pp. 1636-1642, 1982.
[34] V. L. Olson, G. L. Smidt, and R. C. Johnson, "The maximum torque generated by the eccentric, isometric, and concentric contractions of the hip abductor muscles," *Physical Therapy*, vol. 52, pp. 149-158. 1972.
[35] T. D. Cahalan, M. E. Johnson, S. Liu, and E. Y. S. Chao, "Quantitative measurements of hip strength in different age groups," *Clin. Orthop. Rel. Res.*, vol. 246, pp. 136-145, 1989.
[36] G. N. Scudder, "Torque curves produced at the knee during isometric and isokinetic exercises," *Arch. Phys. Med. Rehabil.*, vol. 61, pp. 68-72, 1980.
[37] E. Marsh, D. Sale, A. J. McComas, and J. Quinlan, "Influence of joint position on ankle dorsiflexion in humans," *J. Appl. Physiol.: Respirat. Environ. Exer. Physiol.*, vol. 51, pp. 160-167, 1981.
[38] H. Tropp, "Pronator muscle weakness in functional instability of the ankle joint," *Int. J. Sports Med.*, vol. 7, pp. 291-294, 1986.
[39] L. Root, S. R. Miller, and P. Kirz, "Posterior tibial-tendon transfer in patients with cerebral palsy," *J. Bone and Joint Surg.*, vol. 69-A, pp. 1133-1139, 1987.
[40] E. E. Bleck, *Orthopaedic management in cerebral palsy*. Philadelphia, PA: Mac Keith, 1987, ch. 7, pp. 213-282.
[41] L. G. Hallen and O. Lindahl, "The screw home movement in the knee-joint," *Acta Orthop. Scand.*, vol. 37, pp. 97-106, 1966.
[42] S. Siegler, J. Chen, and C. D. Schneck, "The three-dimensional kinematics and flexibility characteristics of the human ankle and subtalar joints—part I: kinematics," *J. Biomech. Eng.*, vol. 110, pp. 364-373, 1988.
[43] R. H. Jensen and D. T. Davy, "An investigation of muscle lines of action about the hip: a centroid line approach vs the straight line approach," *J. Biomech.*, vol. 8, pp. 103-110, 1975.
[44] J. R. Gage, J. Perry, R. R. Hicks, S. Koop, and J. R. Werntz, "Rectus femoris transfer as a means of improving knee function in cerebral palsy," *Development. Med. Child Neurol.*, vol. 29, pp. 159-166, 1987.

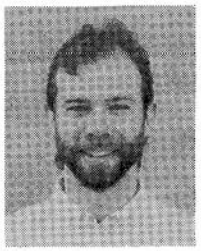

Scott L. Delp received the B.S. degree in mechanical engineering from Colorado State University, Fort Collins, in 1983, the M.S. degree in mechanical engineering from Stanford University, Stanford, CA, in 1986, and expects to receive the Ph.D. degree in mechanical engineering from Stanford University in 1990.

He worked at Hewlett Packard's Engineering Workstation Division in Fort Collins, CO, from 1983-1985, and has been with the VA Rehabilitation R & D Center in Palo Alto, CA since 1986. His research interests are design automation, surgery simulation, and dynamic analysis of human movement.

Mr. Delp is a member of the American Society of Biomechanics, the International Society of Biomechanics, and ASME.

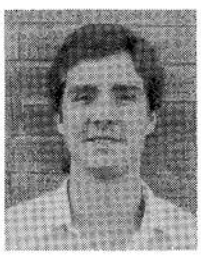

J. Peter Loan received B.S. degrees in philosophy and mechanical engineering from the Massachusetts Institute of Technology, Cambridge, in 1986, and M.S. degrees in mechanical engineering and computer science from Stanford University, Stanford, CA, in 1988 and 1989, respectively.

He is currently a Biomedical Engineer at the Rehabilitation R & D Center at the Palo Alto VA Medical Center. His current research interests include computer graphics and simulation of biomechanical systems.

Melissa G. Hoy received the B.A. degree in dance from the University of Colorado, Boulder, in 1976 and the M.S. and Ph.D. degrees in kinesiology from the University of California, Los Angeles, in 1980 and 1984, respectively.

She is currently a Health Research Scientist at the Rehabilitation R & D Center at the Palo Alto VA Medical Center. Her current research interests are dynamics of human movement, motor control, and surgery simulation.

Dr. Hoy is a member of the American Society of Biomechanics and the Society of Neuroscience.

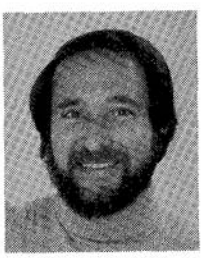

Felix E. Zajac (M'70) was born in Baltimore, MD. He received the B.E.E. degree from Rensselaer Polytechnic Institute, Troy, NY, in 1962, and the M.S. degree in electrical engineering and the Ph.D. degree in neurosciences from Stanford University, Stanford, CA, in 1965 and 1968, respectively.

From 1968-1970, he was Staff Associate, Laboratory of Neural Control, National Institutes of Health. From 1970-1979, he was on the Electrical Engineering faculty, University of Maryland, and was Chairman, Biomedical Engineering Program, and Director, Biomedical Research Laboratory. Since 1979, he has been with the Palo Alto VA Rehabilitation R & D Center, and is now Director of this Center, and on the faculty of Stanford University (Professor of Mechanical Engineering, Research, and Member, Neurosciences Program). His past research involved the study of the properties of motor units. He currently studies the muscular coordination and dynamics of multiarticular movement in abled and disabled persons.

Dr. Zajac was the recipient of the IEEE Control Society (Bay Area Chapter) Outstanding Achievement Award in Control Engineering in 1983. He has served as a Regular Study Section Member and in other advisory capacities to the National Institutes of Health, and currently holds a NIH Javits Neuroscience Investigator Award.

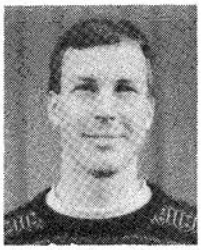

Eric L. Topp received the B.S. degree in mechanical engineering from the University of New Mexico, Albuquerque, in 1980 and the M.S. degree in mechanical engineering from Stanford University, Stanford, CA, in 1983.

He is currently a Biomedical Engineer at the Palo Alto VA Medical Center. His research interests include dynamics of human movement, and computer modeling and simulation of locomotor mechanics.

Mr. Topp is a member of the Association for Computing Machinery.

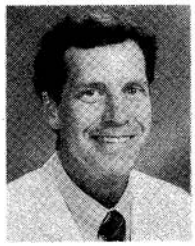

Joseph M. Rosen received the B.A. degree in biology from Cornell University, Ithaca, NY, in 1974 and the M.D. degree from Stanford University, Stanford, CA, in 1978.

After completing specialty training in reconstructive and plastic surgery at Stanford in 1985, he became an Assistant Professor of Surgery at Stanford. In 1989 he was appointed as the Medical Director of the Rehabilitation R & D Center at the Palo Alto VA Medical Center. He is interested in nerve repair, man-machine interaction, and surgery simulation.

Dr. Rosen is a member of the Plastic Surgery Research Council and a candidate member of the Plastic Surgery Society.